ORIGINAL PAPER

Towering and internal rogue waves induced by two-layer interaction in non-uniform fluid. A 2D non-autonomous gCDGKSE

H. I. Abdel-Gawad

Abstract A Generalized (2+1)-dimensional Caudrey–Dodd–Gibbon–Kotera–Sawada equation (2D-gCDGKSE) is an integro-differential equation that describes tow-layer fluid interaction. The non-autonomous (2+1)-dimensional gCDGKSE (NAUT-gCDGKSE) was rarely considered in the literature. In the previous works, the concepts of two-layer fluid interaction and non-uniform fluid were not explored. This motivated us to focus the attention on these themes. Our objective is to inspecting waves structures in non-uniform fluid which describes fluid flows near a solid boundary. Thus, the present work is completely new. Our objective, here, is to inspect waves which are similar to those created in waterfall, water waves behind dams, boat sailing, in the network of canals during water release, and internal waves in submarine. In a uniform fluid, rogue waves occur in open oceans and seas, while in the present case of non-uniform fluid, towering and internal rogue waves occur near barriers (islands) and near submarine, respectively. This was consolidated experimentally, as it was shown that rogue wave is produced in a water tank (which is with solid boundary). The exact solutions of NAUT-gCDGKSE are derived here, by implementing the extended unified method (EUM). In applications, it is found that the EUM is of lower time cost in symbolic computation, than when using Lie symmetry, Darboux and Auto- Bucklund transformations. The results obtained here are evaluated numerically, and they are displayed in graphs. They reveal multiple waves structures with relevance to waves created near a solid boundary. Among them are towering and internal rogue waves, internal (hollowed) and bulge-U-shape wave and S-shape wave, water fall, saddle wave, and dromoions.

Keywords Non-autonomous · Caudrey–Dodd–Gibbon–Kotera–Sawada equation · Towering · Internal · Rogue waves · Waterfall

1 Introduction

Indeed, the Caudrey–Dodd–Gibbon–Kotera–Sawada equation (CDGKSE) and the generalized CDGKSE (gCDGKSE) describe two-layer fluid interaction. The gCDGKSE was currently considered in the literature. It is a higher-order generalization of the celebrated Kadomtsev–Petviashvili equation. In [1], a (2+1)-dimensional gCDGKS equation (2D-gCDGKSE) was studied by the Hirota bilinear method (HBM). A hierarchy of bilinear CDGKSE with a unified structure and a nonlinear superposition formula was proved under certain conditions [2]. Under the HBM, the specific expression for N-soliton solutions of 2D-gCDGKSE in fluid mechanics was given [3]. In [4], the 2D- CDGKS-like equation was investigated, based on bilinear neural network method, where novel solutions were derived. The N-soliton solutions were found by focusing on the

H. I. Abdel-Gawad (✉)
Mathematics Department, Faculty of Science, Cairo University, Giza, Egypt
e-mail: hamdyig@yahoo.com

nonlinear superposition between one lump and other types of localized waves of the 2D-gCDGKSE [5]. By means of the HBM, lump-type solution and two types of interaction solutions of the 2D-Caudrey–Dodd–Gibbon–Kotera–Sawada equation were obtained [6]. The interaction phenomenon between the lump waves and stripe solitons in the 2D- CDGKSE, by making use of the HBM, was investigated [7]. The CDGKS hierarchy associated with a matrix spectral problem was suggested, based on Lenard recursion equations [8]. In [9], Bernoulli sub-equation function method was applied to obtain some new exact oscillating solutions. The CDGKSE was analytically investigated by using the HBM, where N-soliton solution was derived [10]. In [11], M-lump and interaction between lumps and kink solitons of the 2D- CDGKSE were studied based on HBM. Novel analytical and numerical solutions of the CDGKSE were established by means of Tanh method and order residual power series method [12]. The HBM was used to obtain some breather wave and lumps solutions to the CDGKSE that was converted into its potential version together with implementing of Cole–Hopf transformation [13]. The Lie symmetry analysis, exact solutions, and conservation laws to the time fractional CDGKSE with Riemann–Liouville derivative were investigated [14]. The solution of the third-order isospectral equation of the CDGKSE for soliton potential was obtained recursively from the Riccati equation via the auto-Backlund transformation [15]. The symmetry transformations of the 2D- CDGKSE with Lou's direct method that based on Lax pairs were considered [16]. The Bäcklund transformation and Lax pair for a differential–difference CDGKSE were presented in [17]. The HBM of 2D- CDGSKE was used to obtain, a class of solutions, among them, lump, strip soliton, a pair of resonance solitons as well as the rogue wave [18]. A 2D- CDGKSE was investigated with the help of the HBM, where some singular soliton, shock-wave, breather-stripe soliton, and hybrid solutions were found [19]. In [20], the HBM combined with the simplified Hereman method was used to determine the N-soliton solutions for the fifth-order CDG equation. Some works related to the present work on CDGKSE with variable coefficients (VCs) have received the attention of many research works. The interaction between solitons and the cnoidal periodic waves of the 2D- CDGKSE was explored via the consistent Tanh expansion [21].The Darboux transformation, associated with nonlocal symmetry of the 2D- CDGKSE, was localized by introducing four field quantities [22]. It is worthy to mention the CDGKSE with variable coefficients is modestly studied in the literature. In [23], soliton solutions of the 2D- VCs-CDGKSE were derived via a new velocity resonance condition. The (2+1)-dimensional variable-coefficient CDGKSE was studied, and N-th-order Pfaffian solutions were constructed [24]. In [25], the HBM was used to derive M-lump solution and N -soliton solution to the 2D- VCs-CDGKSE. Multi-waves and breathers solution of the 2D- VCs-CDGKSE, under the HBM, were obtained [26]. In [27], the bilinear form, bilinear Bäcklund transformation, and Lax pair of a 2D-VCs-CDGKSE were derived via Bell polynomials. The HBM was employed to study the 2D- VCs-CDGKSE [28].In these works, the studies focused on waves generated in a uniform fluid, while the notions of nonuniform fluid and the two-layer fluid interaction were not invoked there. In contrast with this, here, these characteristics are dealt with. The solitary wave ansatz method along with HBM and numerical simulations was used to study the CDGKSE and its bidirectional form [29,30]. An algebraic method with symbolic computation was employed to construct a series of exact solutions of the 2D-CDGKSE [31]. Based on bilinear neural network method, the lump solutions were constructed by activation functions in the single hidden layer neural network model and the "3-2-2" neural network model [32]. The bilinear residual network method was proposed to solve the steady state CDGKSE, where rogue waves were shown [33]. After the graphs displayed in [33], they show peak waves and not rogue waves. We think that rogue waves are produced in a system, when it is in the unsteady state. Some relevant works were also carried in [34,35].

The NAUT- DGKSE (with time-dependent coefficients) describes waves in nonuniform fluid, where the velocity is space dependent at a fixed time. It characterizes every fluid flows near a solid boundary. Thus, waterfall, water waves behind dams, and water flow in the network of canals during water release are nonuniform fluid flow. Here, a (2+1)-dimensional - NAUT-gCDGKSE is considered. So, we are concerned with inspecting waves in nonuniform flow. The exact solutions are found here via the extended unified method (EUM) [36–40]. Further papers on the neural network method were carried [41,42]. Some works on rogue waves and dynamical fluid equations were presented [43–50].

The outlines of this paper are as follows. In Sect. 2, the model equation and a brief account of the EUM are presented. Section 3 is devoted to polynomial solutions, while rational solutions are given in Sect. 4. Section 5 is concerned with discussions, while some conclusions are given in Sect. 6

2 The model equation and outlines of EUM

2.1 The model equation

The $(2 + 1)$-dimensional gCDGKSE was considered in [1],

$$36u_t + (u_{xxxx} + 15uu_{xx} + 15u_{xxx})_x - \alpha \int u_{yy} dx \\ - \gamma (u_{xxy} + 3uu_y + 3u_x \int u_y dx) = 0, \tag{1}$$

where $u = u(x, y, t)$ is the wave function ; α and γ are real parameters. In (1), we put $v = \int u_y dx$, so, (1) reduces to

$$36u_t + (u_{xxxx} + 15uu_{xx} + 15u_{xxx})_x - \alpha v_y \\ - \gamma (u_{xxy} + 3uu_y + 3u_x v) = 0, \tag{2}$$
$$v_x = u_y.$$

A more general CDGKSE is proposed, here, by

$$\beta_1 u_t + \nu \left(u_{xxxx} + \beta_2 uu_{xx} + \beta_2 u^3 \right)_x \\ - \alpha v_y - \gamma \left(u_{xxy} + \beta_3 uu_y + \beta_3 u_x v \right) = 0, \tag{3}$$
$$v_x = u_y.$$

In (3), when $\beta_1 = 36$, $\beta_2 = 15$, $\beta_3 = 3$, $\nu = 1$, then (3) reduces to (2). As, we are interested in studying non-autonomous gCDGKSE, we consider (3) with time-dependent coefficients

$$\beta_1 u_t + \nu(t) \left(u_{xxxx} + \beta_2 uu_{xx} + \beta_2 u^3 \right)_x \\ - \alpha(t)v_y - \gamma(t) \left(u_{xxy} + \beta_3 uu_y + \beta_3 u_x v \right) = 0, \tag{4}$$
$$v_x = u_y.$$

Equation (4) suggests to introduce a stream function $\psi(x, y, t)$ such that $u = \psi_x$ and $v = \psi_y$, and it reduces to the closed form

$$-\alpha(t)\psi_{yy} + \beta_1 \psi_{xt} - \gamma(t) \\ \left(\beta_3 \left(\psi_x \psi_{xy} + \psi_y \psi_{xx} \right) + \psi_{xxxy} \right) \\ + \nu(t) \left(\beta_2 \left(3\psi_x^2 \psi_{xx} + + \psi_{xx}\psi_{xxx} + \psi_x \psi_{xxxx} \right) \\ + \psi_{xxxxxx} \right) = 0. \tag{5}$$

In (5), we consider the similarity transformations $\psi(x, y, t) = \varphi(z, t), z = \mu(t)x + \sigma(t)y$, and $t =$

t, where z and t are independent variables. Thus, (5) becomes

$$-\beta_1 \mu(t)\varphi - \alpha(t)\sigma(t)^2 \varphi_{zz} \\ - \gamma(t)\mu(t)^2 \sigma(t) \left(2\beta_3 \varphi_z \varphi_{zz} + \mu(t)\varphi_{zzzz} \right) \\ + \nu(t) \left(\beta_2 \mu(t)^4 \left(3\varphi_z^2 \varphi_{zz} + \varphi_{zz}\varphi_{zzz} + \mu(t)\varphi_z \varphi_{zzzz} \right) \right) \\ + \mu(t)^6 \varphi_{zzzzzz} = 0. \tag{6}$$

The exact solutions of (6) are found, here, by using the EUM.

2.2 Outlines of the EUM

Consider the NLPDE's , with explicit time-dependent

$$f(t, u_x, u_y, u_z u_t, v_x, v_y, v_z v_t, u_{xx}, ...) = 0. \tag{7}$$

We introduce the similarity transformations $u(x, y, z, t) = U(z, t), z = \alpha(t)x + \beta(t)y$, and $t := t$; thus, (7) is rewritten as

$$F(t, U_t, U_z, U_{tt}, U_{zz}, ...) = 0. \tag{8}$$

The EUM asserts that the solutions of (6) are expressed in polynomial and rational forms in an auxiliary function that satisfies suitable auxiliary equations. It is worthy to mention that the EUM can be considered as an alternative technique to the use of Lie group symmetries of NLPDEs. In the application, it is found that the use of the EUM is of lower time cost, in symbolic computations, than the Lie symmetry. So we think that it prevails the use of Lie symmetries as the later technique requires a long hierarchy of steps. On the other hand, it provides a wide class of solutions.

2.2.1 Polynomial solutions

The polynomial solutions of (6) are expressed in the form

$$\varphi(z, t) = \sum_{j=0}^{j=n} a_j(t) g(z, t)^j,$$
$$(g_z(z, t))^p = \mu \sum_{j=0}^{j=pk} c_j g(z, t)^j,$$
$$(g_t(\xi, z, t))^p = h(t) \sum_{j=0}^{j=pk} c_j g(z, t)^j, p = 1, 2. \tag{9}$$

The solutions in (9) exist if there exist integers n, and k. Thus, our objective is to show that there exist

integers n, and k with relevance to (6). For achieving this, we use two conditions: the balance and consistency conditions. We consider the case when $p = 1$. By inserting (9) into (7), we find that the balance condition gives rise to $n = k - 1$. For the consistency condition, we need to calculate:

(i) The number of equations that results from inserting Eq. (7) into Eq. (4) and by setting the coefficients of $g(z, t)^i$, $i = 0, 1, 2, .. etc.$ equals to zero; $r(k) = 7k - 6$.

(ii) The number of arbitrary functions and parameters in Eq. (7), namely c_i, $a_i(z, t)$, $s(k) = 2k + 1$.

Together with using the condition $r(k) - s(k) \leq q$, where q is the highest order derivative in (6) ($q = 6$), the last conditions lead to $1 \leq k \leq 13/5$.

When $p = 2$, the same results hold. We mention that the solutions of Eq. (7) are hyperbolic functions when $p = 1$., while, when $p = 2$, they are periodic or elliptic functions.

2.2.2 Rational forms

The rational solutions of Eq. (6) are expressed in the form

$$U(z, t) = A(t)\frac{a_1 g(z, t) + a_0}{s_1 g(z, t) + s_0}, \tag{10}$$

$$\begin{aligned}(g_z(z, t))^p &= \sum_{j=0}^{j=pk} c_j g(z, t)^j, \\ (g_t(z, t))^p &= h(t) \sum_{j=0}^{j=pk} c_j g(z, t)^j, \quad p = 1, 2.\end{aligned} \tag{11}$$

3 Polynomial solutions of (6)

3.1 When $p = 1, k = 2, n = 1$

In this case, we write

$$\varphi(z, t) = a_1(t)g(z, t) + a_0(t), \tag{12}$$

and the auxiliary equations (AEs) are

$$\begin{aligned}g_z(z, t) &= c_2 g(z, t)^2 + c_1 g(z, t) + c_0, \\ g_t(z, t) &:= h(t) \left(c_2 g(z, t)^2 + c_1 g(z, t) + c_0\right).\end{aligned} \tag{13}$$

Inserting (12) and (13) into (6) and by setting the coefficients of $g(z, t)^j$, $j = 0, 1, 3, ...$, equal to zero lead to

$\mu(t) = r, \; a_1(t)$

$$= -\frac{c_2 \left(\sqrt{\beta_2 \left(\beta_2(2r + 1)^2 - 120r^2\right)} + \beta_2(2r + 1)\right)}{\beta_2},$$

$$\sigma(t) = \frac{1}{K} \left(r^2 c_1^2 - 4c_0 c_2 \beta_2 \left(\sqrt{\beta_2(\beta_2(2r + 1)^2 - 120r^2)}\right.\right.$$

$$+ \beta_2 \left(2r^2 + 3r + 1\right)$$

$$\left.\left. -60r^2 + r\sqrt{\beta_2(\beta_2(2r + 1)^2 - 120r^2)}\right) v(t)\right),$$

$$K = 2 \left(\beta_3 \sqrt{\beta_2(\beta_2(2r + 1)^2 - 120r^2)}\right.$$

$$\left. + \beta_2 \left(\beta_3(2r + 1) - 6r\right)\right) \gamma(t),$$

$$h(t) = \frac{1}{M}(\sqrt{\beta_2(\beta_2(2r + 1)^2 - 120r^2)}(\left(c_1^2 - 4c_0 c_2\right)^2$$

$$- r^3 v(t) \left(-4\beta_3 r^2 \left(\beta_3(2r + 1) + 9r\right) \gamma(t)^2\right.$$

$$+ 2\beta_2 r(r + 1)) ((\beta_3(2r + 1) - 3r)\gamma(t)^2 - 30r\alpha(t)v(t)$$

$$+ \beta_2^2(r + 1)^2(2r + 1)\alpha(t)v(t))) - r^3 \left(c_1^2 - 4c_0 c_2\right)^2 v(t)$$

$$\left(240\beta_3^2 r^4 \gamma(t)^2 + \beta_2^3(2r^2 + 3r + 1)^2 \alpha(t)v(t)\right.$$

$$- 4\beta_2(r^2(-72r^2 + 3\beta_3(16r + 13)r$$

$$+ \beta_3^2(2r + 1)^2))\gamma(t)^2 - 450r^4\alpha(t)v(t))$$

$$+ 2\beta_2^2 r(r + 1) ((2r + 1) (\beta_3(2r + 1)$$

$$\left.\left. -3r) \gamma(t)^2 - 30r(3r + 2)\alpha(t)v(t)\right)\right),$$

$$M = (8\beta_1\beta_3^2 r\gamma(t)^2 - 24\beta_1\beta_3 r\gamma(t)^2$$

$$+ 4\beta_1\beta_3^2 \gamma(t)^2)\sqrt{\beta_2(\beta_2(2r + 1)^2 - 120r^2)}$$

$$- 240\beta_1\beta_3^2 r^2\gamma(t)^2 + 16\beta_1\beta_2\beta_3^2 r^2\gamma(t)^2$$

$$+ 72\beta_1\beta_2 r^2\gamma(t)^2 - 48\beta_1\beta_2\beta_3 r^2\gamma(t)^2$$

$$+ 16\beta_1\beta_2\beta_3^2 r\gamma(t)^2 - 24\beta_1\beta_2\beta_3 r\gamma(t)^2$$

$$+ 4\beta_1\beta_2\beta_3^2\gamma(t)^2. \tag{14}$$

The solution of (5) (or (6)) is

$$\psi(x, y, t) = \frac{1}{2\beta_2}\sqrt{\beta_2(\beta_2(2r + 1)^2 - 120r^2)}$$

$$+ \beta_2(2r + 1) \left(\sqrt{c_1^2 - 4c_0 c_2}\right.$$

$$+ c_1 \text{Tanh}\left[\frac{1}{2M}\sqrt{c_1^2 - 4c_0 c_2} (rx + B(t)\right.$$

$$+ (r^2 y c_1^2 - 4c_0 c_2\beta_2 (-60r^2$$

$$+ \beta_2 \left(2r^2 + 3r + 1\right)$$

$$\left.\left. + \sqrt{\beta_2(\beta_2(2r + 1)^2 - 120r^2)}(r + 1)\right) v(t)\right)\right) + a_0(t),$$

$$M = 2 \left(\beta_3\sqrt{\beta_2 \left(\beta_2 (2r + 1)^2 - 120r^2\right)}\right.$$

$$\left. + \beta_2 \left(\beta_3(2r + 1) - 6r\right)) \gamma(t)\right),$$

$$B(t) = \int_0^t h(s)ds, \tag{15}$$

where $h(t)$ is given in (14).

The two-layer solutions are $u = \psi_x$ and $v = \psi_y$, and they are

$$u(x, y, t) = \frac{1}{4\beta_2} r \operatorname{Sech}\left[\frac{1}{2M}\sqrt{c_1^2 - 4c_0 c_2}\ (rx + B(t)\right.$$
$$+ \left(\left(c_1^2 - 4c_0 c_2\right) r^2 y\ \beta_2\left(\sqrt{\beta_2\left(\beta_2(2r+1)^2 - 120r^2\right)}(r+1)\right.\right.$$
$$+ \beta_2\left(2r^2 + 3r + 1\right) - 60r^2\right) v(t))]^2\right)\left(c_1^2 - 4c_0 c_2\right)$$
$$\left(\sqrt{\beta_2\left(\beta_2(2r+1)^2 - 120r^2\right)} + \beta_2(2r+1)\right), \tag{16}$$

$$v(x, y, t) = \frac{1}{4M}\left(r^2 \operatorname{Sech}\left[\frac{1}{2M}\sqrt{c_1^2 - 4c_0 c_2}\ (rx + B(t)\right.\right.$$
$$+ \left(r^2 y(c_1^2 - 4c_0 c_2)\ \beta_2\left((r+1)\sqrt{\beta_2\left(\beta_2(2r+1)^2 - 120r^2\right)}\right.\right.$$
$$+ \beta_2\left(2r^2 + 3r + 1\right) - 60r^2\right) v(t))]^2\left(c_1^2\right.$$
$$- 4c_0 c_2\right)^2\left(\sqrt{\beta_2\left(\beta_2(2r+1)^2 - 120r^2\right)}\right.$$
$$+ \beta_2(2r+1))\left((r+1)\sqrt{\beta_2\left(\beta_2(2r+1)^2 - 120r^2\right)}\right.$$
$$+ \beta_2\left(2r^2 + 3r + 1\right) - 60r^2\right) v(t)\right). \tag{17}$$

The solutions in (16) and (17) are displayed for the two-layer functions u and v in Figs. 1 (i)-(vi).

3.2 When $p = 1, k = 3$ and $n = 2$

The solution of (6) and the AEs are

$$\varphi(z, t) = a_2(t)g(z, t)^2 + a_1(t)g(z, t) + a_0(t),$$
$$g_z(z, t) = c_3 g(z, t)^3 + c_2 g(z, t)^2 + c_1 g(z, t) + c_0,$$
$$g_t(z, t) := h(t)\left(c_3 g(z, t)^3 + c_2 g(z, t)^2 + c_1 g(z, t) + c_0\right). \tag{18}$$

From (18) into (6), it gives rise to

$$a_2(t) = -\frac{2\left(\sqrt{30}\sqrt{\beta_2} - 30\right)c_3}{\beta_2 - 30},$$

$$a_1(t) = \frac{20\left(27\sqrt{30}\beta_2^{3/2} - 16\beta_2^2 + 450\beta_2 - 1410\sqrt{30}\sqrt{\beta_2} + 18900\right)c_2}{(\beta_2 - 30)\left(8\sqrt{30}\beta_2^{3/2} - 165\beta_2 - 390\sqrt{30}\sqrt{\beta_2} + 9450\right)},$$

$$\mu(t) = \frac{\sqrt{30}\sqrt{\beta_2} - \beta_2}{2(\beta_2 - 30)},$$

$$c_0 = \frac{9c_1 c_2 c_3 - 2c_2^3}{27c_3^2},$$

$$\sigma(t) = \frac{P}{Q}, \quad P = (c_2^2 - 3c_1 c_3)^2 \beta_2^2$$
$$\left(-13020304500000\sqrt{30}\sqrt{\beta_2}\right.$$
$$+ 40312424250000\beta_2$$
$$+ 5063451750000054340875 0000\beta_2^2$$

$$-1919359800000\sqrt{30}\beta_2^{3/2} + 72994770000\sqrt{30}\beta_2^{5/2}$$
$$+ 876582000\sqrt{30}\beta_2^{7/2} - 100068615000\beta_2^3$$
$$- 48431250\sqrt{30}\beta_2^{9/2}$$
$$+ 331560\sqrt{30}\beta_2^{11/2} + 1024\sqrt{30}\beta_2^{13/2}$$
$$- 186240\beta_2^6 + 7159725\beta_2^5 + 1561092750\beta_2^4)v(t),$$

$$Q = 18c_3^2(\beta_2 - 30)^2(128\sqrt{30}(16\beta_3 - 195)\beta_2^{11/2}$$
$$+ 6144\beta_2^6 + 3375634500000\beta_3 3061800000\beta_2(421\beta_3$$
$$- 630) - 16074450000\sqrt{30}\sqrt{\beta_2}(40\beta_3 - 21)$$
$$+ 105\sqrt{30}(976\beta_3 + 26625)\beta_2^{9/2} - 240(1040\beta_3$$
$$- 1281)\beta_2^5 - 378000(947\beta_3 - 18714)\beta_2^3$$
$$- 1620000\sqrt{30}\beta_2^{3/2} - 12600\sqrt{30}(3494\beta_3 + 2841)\beta_2^{7/2}$$
$$+ 3150(8875\beta_3 - 41928)\beta_2^4 + 27000\sqrt{30}(87332\beta_3$$
$$- 177483)\beta_2^{5/2} - 810000(59161\beta_3 + 76260)\beta_2^2$$
$$+ (12710\beta_3 - 79569))$$
$$\gamma(t), \tag{19}$$

and there exists an equation for $h(t)$, which is very lengthy to be produced here.

The solution of (5) is

$$\psi(x, y, t) = \frac{1}{M}\left(10c_2^2(e^{2c_1(B(t)+z)}\right.$$
$$+ e^{\frac{2c_2^2(B(t)+z)}{3c_3}})(4e^{2c_1(B(t)+z)} - e^{\frac{2c_2^2(B(t)+z)}{3c_3}}$$
$$- 2e^{2c_1(B(t)+z)})(27\sqrt{30}\beta_2^{3/2} - 16\beta_2^2 + 450\beta_2$$
$$- 1410\sqrt{30}\sqrt{\beta_2} + 18900) - 90c_1 c_3(e^{4c_1(B(t)+z)}$$
$$+ e^{\frac{2(c_2^2 + 3c_1 c_3)(B(t)+z)}{3c_3}})(27\sqrt{30}\beta_2^{3/2} - 16\beta_2^2$$
$$+ 450\beta_2 - 1410\sqrt{30}\sqrt{\beta_2} + 18900)$$
$$+ 20c_2\left(e^{2c_1(B(t)+z)} - e^{2c_1(B(t)+z)}\right)$$
$$e^{c_1(B(t)+z)}\sqrt{(c_2^2 - 3c_1 c_3)(e^{2c_1(B(t)+z)} + e^{\frac{2c_2^2(B(t)+z)}{3c_3}})}$$
$$(-81\sqrt{10}\beta_2^{3/2} + 16\sqrt{3}\beta_2^2 - 450\sqrt{3}\beta_2$$
$$+ 4230\sqrt{10}\sqrt{\beta_2} - 18900\sqrt{3})$$
$$+ 3\left(e^{\frac{2c_2^2(B(t)+z)}{3c_3}} + e^{2c_1(B(t)+z)}\right)^2 c_3 \beta_2$$
$$- 30\left(9450 - 390\sqrt{30}\sqrt{\beta_2}\right.$$
$$8\sqrt{30}\beta_2^{3/2} - 165\beta_2\right)a_0(t)\right),$$

$$M = 3(\beta_2 - 30)c_3(e^{\frac{2c_2^2(B(t)+z)}{3c_3}} + e^{2c_1(B(t)+z)})^2,$$

$$z = y\sigma(t) + \frac{\left(\sqrt{30}\sqrt{\beta_2} - \beta_2\right)x}{2(\beta_2 - 30)},$$
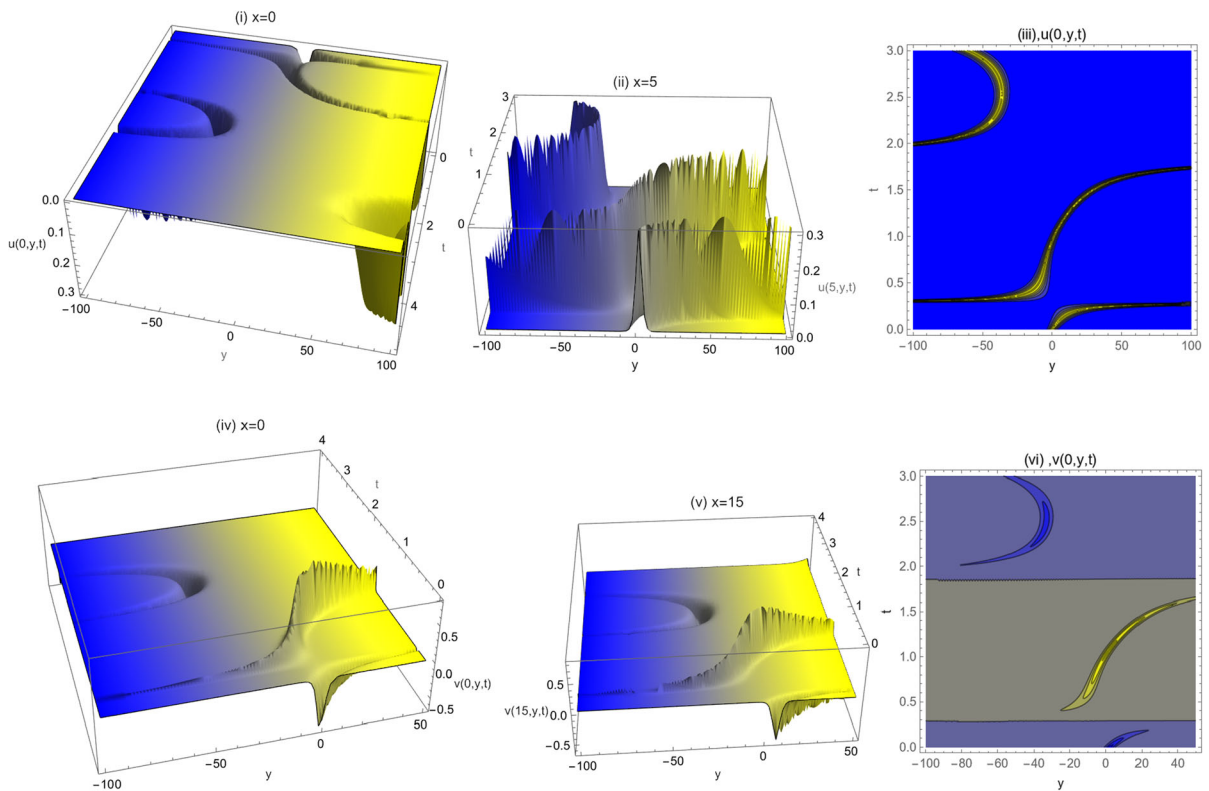
$$B(t) = \int_0^t h(s)ds, \tag{20}$$

Fig. 1 Figure 1 (i)–(vi). The 3D and contour plots of u and v are displayed against y and t for two values of x, in Figs.1(i)–(iii) and 1(v)–(vi), respectively. When $\alpha(t) = 3\sin(2(t-2))$, $\nu(t) = e^{-0.5t}\sin(2(t-5))(\cos(2(t-2))+2)$, $\gamma(t) = \sqrt{\cos(2(t-2))+2}$, $\beta_2 = 5$, $r = 0.25$, $c_1 = 2.5$, $c_0 = 0.7$, $c_2 = 1.5$, $\beta_3 = 0.3$, $\beta_1 = 0.2$.

Figure 1(i) shows double-U-shape internal (hollowed waves). Figure 1(ii) shows U-shape and S-shape bulge waves. Figure 1 (iii) shows the same waves.

Figure 1(iv) shows U-shape internal (hollowed wave) and S-shape bulge wave. Figure 1(v) and (vi) shows the same behavior.

where $\sigma(t)$ and $h(t)$ are given in (19). By bearing in mind that $u = \psi_x$ and $v = \psi_y$, it leads to

$$u(x, y, t) = -\frac{1}{N}\left(10\left(\exp\left(\frac{\left(2c_2^2 + 3c_1c_3\right)\left(2(\beta_2 - 30)B(t) - \beta_2(x - 2y\sigma(t)) - 60y\sigma(t) + \sqrt{30}\sqrt{\beta_2}x\right)}{3(\beta_2 - 30)c_3}\right)\right.\right.$$

$$\left.+ \exp\left(\frac{\left(c_2^2 + 6c_1c_3\right)\left(2(\beta_2 - 30)B(t) - \beta_2(x - 2y\sigma(t)) - 60y\sigma(t) + \sqrt{30}\sqrt{\beta_2}x\right)}{3(\beta_2 - 30)c_3}\right)\right)$$

$$\left(c_2^2 - 3c_1c_3\right)^2\sqrt{30} - \sqrt{\beta_2}\sqrt{\beta_2}\left(18900 - 1410\sqrt{30}\sqrt{\beta_2}27\sqrt{30}\beta_2^{3/2} - 16\beta_2^2 + +450\beta_2\right), \tag{21}$$

$$v(x, y, t) = -\frac{20(\beta_2 - 30)}{N} \left(\exp\left(\frac{(2c_2^2 + 3c_1c_3)\left(2(\beta_2 - 30)B(t) - \beta_2(x - 2y\sigma(t)) - 60y\sigma(t) + \sqrt{30}\sqrt{\beta_2}x\right)}{3(\beta_2 - 30)c_3}\right) \right.$$

$$\left. + \exp\left(\frac{(c_2^2 + 6c_1c_3)\left(2(\beta_2 - 30)B(t) - \beta_2(x - 2y\sigma(t)) - 60y\sigma(t) + \sqrt{30}\sqrt{\beta_2}x\right)}{3(\beta_2 - 30)c_3}\right) \right)$$

$$\left(27\sqrt{30}\beta_2^{3/2} - 16\beta_2^2 + 450\beta_2 - 1410\sqrt{30}\sqrt{\beta_2} + 18900\right)\left(c_2^2 - 3c_1c_3\right)^2\sigma(t),$$

$$N = 3(\exp(2c_1(B(t) + y\sigma(t) + \frac{\left(\sqrt{30}\sqrt{\beta_2} - \beta_2\right)x}{2(\beta_2 - 30)})) + \exp(\frac{2c_2^2\left(B(t) + y\sigma(t) + \frac{\left(\sqrt{30}\sqrt{\beta_2} - \beta_2\right)x}{2(\beta_2 - 30)}\right)}{3c_3}))^3$$

$$(\beta_2 - 30)^2\left(8\sqrt{30}\beta_2^{3/2} - 165\beta_2 - 390\sqrt{30}\sqrt{\beta_2} + 9450\right)c_3^2. \tag{22}$$

The solutions in (21) and (22) are displayed for the two-layer functions u and v in Figs.2 (i)-(vii).

3.3 When $p = 2$, $k = 2$ and $n = 1$

Case (i)

We consider (12) and the AEs

$$g_z(z, t) = (m_1 g(z, t) + m_0)\sqrt{c_2 g(z, t)^2 + c_1 g(z, t) + c_0},$$
$$g_t(z, t) := h(t)(m_1 g(z, t) + m_0)\sqrt{c_2 g(z, t)^2 + c_1 g(z, t) + c_0}. \tag{23}$$

From (12) and (18) into 6), we have

$$\mu(t) = -\frac{1}{2}, \quad \sigma(t)$$
$$= \frac{(4c_2^2 m_0^2 + 3c_1^2 m_1^2 - 4c_2 m_1(c_1 m_0 + 2c_0 m_1))\beta_2 v[t]}{64c_2\beta_3\gamma[t]},$$
$$c_0 = \frac{m_0(5c_2 m_0 - 2c_1 m_1)}{m_1^2}, \quad m_1 = -\frac{10c_2 m_0}{c_1},$$
$$a_1(t) = \frac{10\sqrt{30}c_2^{3/2}m_0}{c_1\sqrt{-\beta_2}},$$
$$\beta_2 = -10\beta_3, \quad h(t) = \frac{81c_2^2 m_0^4 v(t)(4\gamma[t]^2 + 25\alpha(t)v(t))}{2\beta_1\gamma[t]^2}. \tag{24}$$

The solution of (6) is

$$\psi(x, y, t) = -\frac{5\sqrt{3}\left(-1 + e^{6(-z + B(t))\sqrt{c_2}m_0}\right)\sqrt{c_2}m_0}{\left(5 + e^{6(-z + B(t))\sqrt{c_2}m_0}\right)\sqrt{\beta_3}}$$
$$+ a_0(t), \quad z = -\frac{x}{2} - \frac{45c_2 m_0^2 v(t)}{2\gamma(t)}y$$
$$B(t) = \int_0^t h(s)ds, \tag{25}$$

where $h(t)$ is given in (24).

The two functions (u and v) solutions are

$$u(x, y, t)$$
$$= -\frac{90\sqrt{3}e^{6\sqrt{c_2}m_0(B(t) + \frac{1}{2}(x + \frac{45yc_2 m_0^2 v(t)}{\gamma(t)}))}c_2 m_0^2}{\left(5 + e^{6\sqrt{c_2}m_0(B(t) + \frac{1}{2}(x + \frac{45yc_2 m_0^2 v(t)}{\gamma(t)}))}\right)^2\sqrt{\beta_3}},$$
$$v(x, y, t)$$
$$= -\frac{4050\sqrt{3}e^{6\sqrt{c_2}m_0(B(t) + \frac{1}{2}(x + \frac{45yc_2 m_0^2 v(t)}{\gamma(t)}))}c_2^2 m_0^4 v[t]}{\left(5 + e^{6\sqrt{c_2}m_0(B(t) + \frac{1}{2}(x + \frac{45yc_2 m_0^2 v(t)}{\gamma(t)}))}\right)^2\sqrt{\beta_3}\gamma[t]}. \tag{26}$$

The two-layer functions u and v, given in (26), are displayed in Fig. 3 (i)-(vi).

Case(ii)

We consider (12) and the AEs

$$g_z(z, t) = \sqrt{m_2 g(z, t)^2 + m_1 g(z, t) + m_0}\sqrt{c_2 g(z, t)^2 + c_1 g(z, t) + c_0},$$
$$g_t(z, t) = h(t)\sqrt{m_2 g(z, t)^2 + m_1 g(z, t) + m_0}\sqrt{c_2 g(z, t)^2 + c_1 g(z, t) + c_0}. \tag{27}$$

From (12) and (27) into (6), it yields

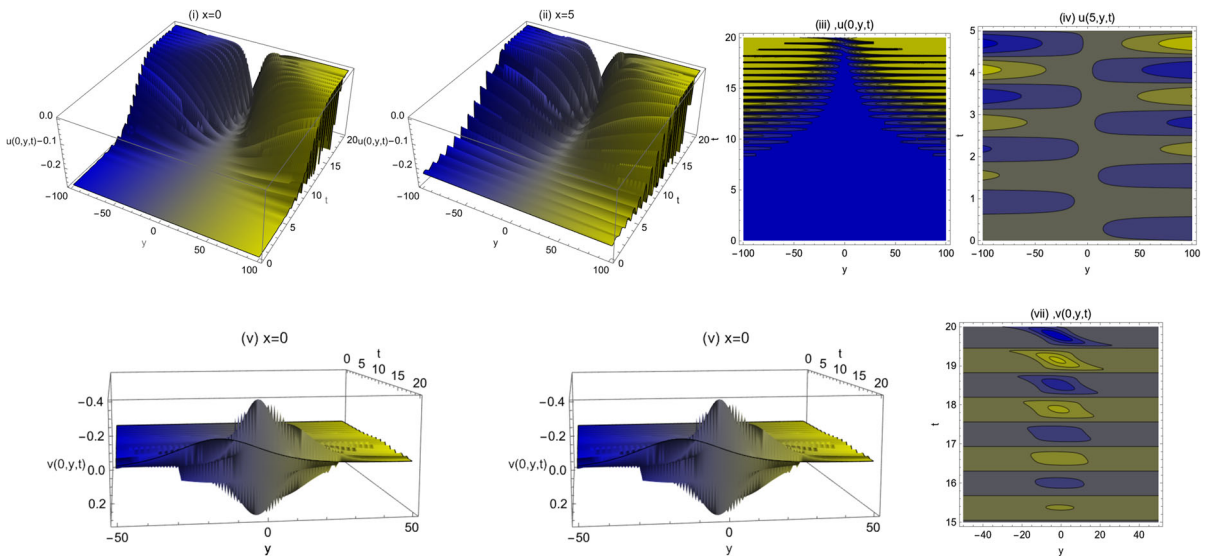**Fig. 2** Figure 2 (i)-(vii). The 3D and contour plots of u and v are displayed against y and t for two values of x, in Fig. 2(i)-(iv) and (v)-(vii), respectively. When $v(t) = 2\sin(5(t-5))$, $\alpha(t) = 3\sin(5(t-5)) + \cos(5(t-5))$, $\beta_3 = 5$, $\beta_1 = 0.2$, $\gamma(t) = 3e^{-0.3t}$, $\beta_2 = 0.1$, $c_1 = 0.05$, $c_3 = 0.025$, $c_2 = 0.5$.

Figure 2(i) and (ii) shows waterfalls. Figure 2(iii) shows the same behavior as in Fig. 2(i) and 2(ii). Figure 2(iv) shows doubly periodic waves.

Figure 2(iv) and (v) shows towering rogue wave and internal rogue wave (in submarine). Figure 2(vii) shows cyclic waves.

where $h(t)$ is given in (28).

The solutions u and v are

$$\mu(t) = -\tfrac{1}{2},$$
$$\sigma(t) = \frac{\beta_2\left(c_2^2\left(3m_1^2 - 8m_0m_2\right) - 2c_2m_2(c_1m_1 + 4c_0m_2) + 3c_1^2m_2^2\right)v(t)}{64\beta_3 c_2 m_2 \gamma(t)},$$
$$m_0 = \frac{m_1^2}{4m_2} - \frac{(c_1^2 - 4c_0c_2)m_2}{4c_2^2},$$
$$m_2 = \frac{c_2 m_1}{c_1}, \quad a_1'(t) = 0, \quad a_1(t) = \frac{\sqrt{30}c_2\sqrt{m_1}}{\sqrt{-\beta_2}\sqrt{c_1}},$$
$$\beta_2 = -10\beta_3,$$
$$h(t) = \frac{(c_1^2 - 4c_0c_2)^2 m_1^2 v(t)\left(25\alpha(t)v(t) + 4\gamma(t)^2\right)}{32\beta_1 c_1^2 \gamma(t)^2}.$$

$$(28)$$

The solution of (5) (or (6)) is

$$\psi(x, y, t) = a_0(t) - \frac{\sqrt{3}\sqrt{m_1}\left(c_1 - \sqrt{c_1^2 - 4c_0c_2}\tanh\left(\frac{\sqrt{c_1^2 - 4c_0c_2}\sqrt{m_1}\left(B(t) - \frac{5(c_1^2 - 4c_0c_2)m_1 yv(t)}{8c_1\gamma(t)} - \frac{x}{2}\right)}{2\sqrt{c_1}}\right)\right)}{2\sqrt{\beta_3}\sqrt{c_1}},$$
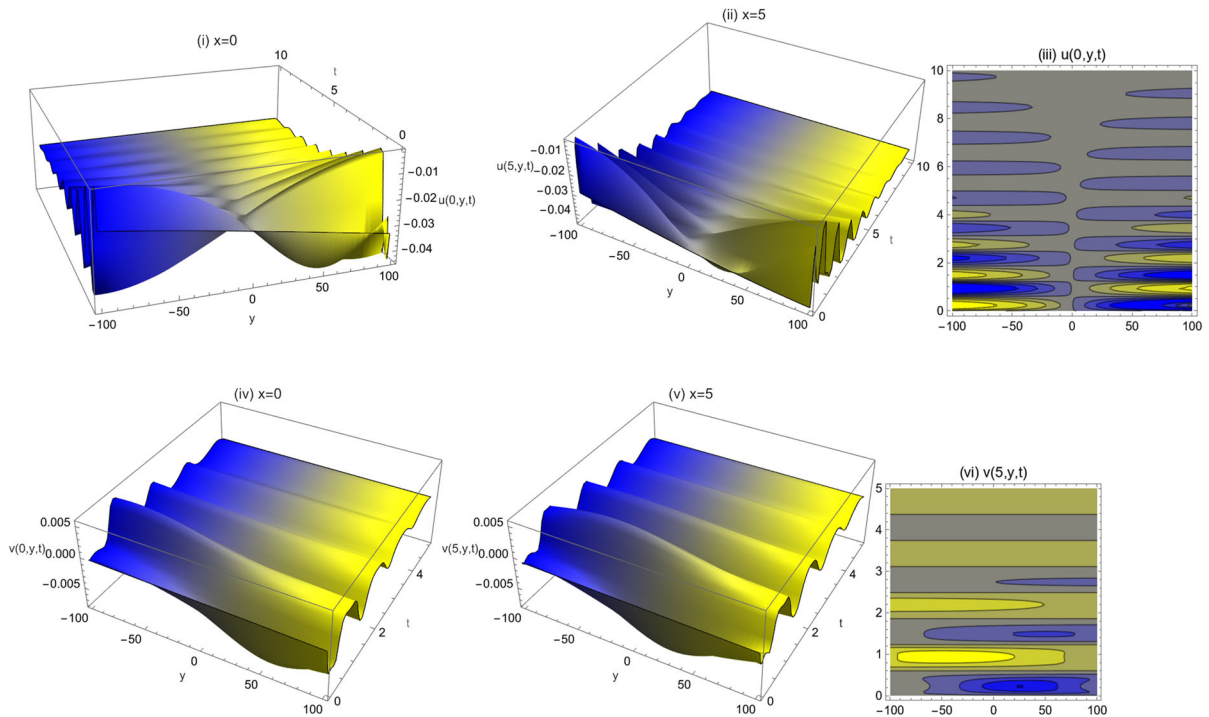$$B(t) = \int_0^t h(s)\,ds,$$

$$(29)$$

Fig. 3 Figure 3 (i)-(vi). The 3D and contour plots of u and v are displayed against y and t for two values of x, in Figs. 3(i)-(iii) and (v)-(vi), respectively. When $v(t) = e^{-0.5t} \sin(5(t - 5))(\cos(5(t - 5)) + 2)$, $\gamma(t) = \sqrt{\cos(5(t - 5)) + 2}$, $\alpha(t) = 3 \sin(5(t - 5))$, $\beta_2 = 5, m_0 = 0.25, c_1 = 2.5, c_2 = 0.05, \beta_3 = 0.3, \beta_1 == 2$.

Figure 3(i) and (ii) shows saddle (Fan waves) with periodic waves tail. Figure (iii) shows saddle waves.
Figure 3(iv) and (v) shows periodic waves cascade. Figure 3(vi) shows the same behavior.

$$u(x, y, t) = -\frac{\sqrt{3}\left(c_1^2 - 4c_0c_2\right)m_1\text{sech}^2(\frac{\sqrt{c_1^2-4c_0c_2}\sqrt{m_1}\left(-B(t)-\frac{5\left(c_1^2-4c_0c_2\right)m_1 yv(t)}{8c_1\gamma(t)}-\frac{x}{2}\right)}{2\sqrt{c_1}})}{8\sqrt{\beta_3}c_1}, \quad (30)$$

$$v(x, y, t) = -\frac{5\sqrt{3}\left(c_1^2 - 4c_0c_2\right)^2m_1^2v(t)\text{sech}^2(\frac{\sqrt{c_1^2-4c_0c_2}\sqrt{m_1}\left(-B(t)-\frac{5\left(c_1^2-4c_0c_2\right)m_1 yv(t)}{8c_1\gamma(t)}-\frac{x}{2}\right)}{2\sqrt{c_1}})}{32\sqrt{\beta_3}c_1^2\gamma(t)}. \quad (31)$$

The two-layer functions u and v, given in (30) and (31), are displayed in Figs. 4 (i)-(vi).

4 Rational solutions of (6).

Here, we consider the solution in (10) together with the AEs in (11).

4.1 When $p = 1$ and k=2

The AEs take the form given in (13), and into (6) it gives

$$\mu(t) = -\frac{\beta_2}{\beta_2 - 30}, \quad A'(t) = 0,$$

$$c_0 = \frac{m(s_0(c_1s_1 - c_2s_0))}{s_1^2},$$

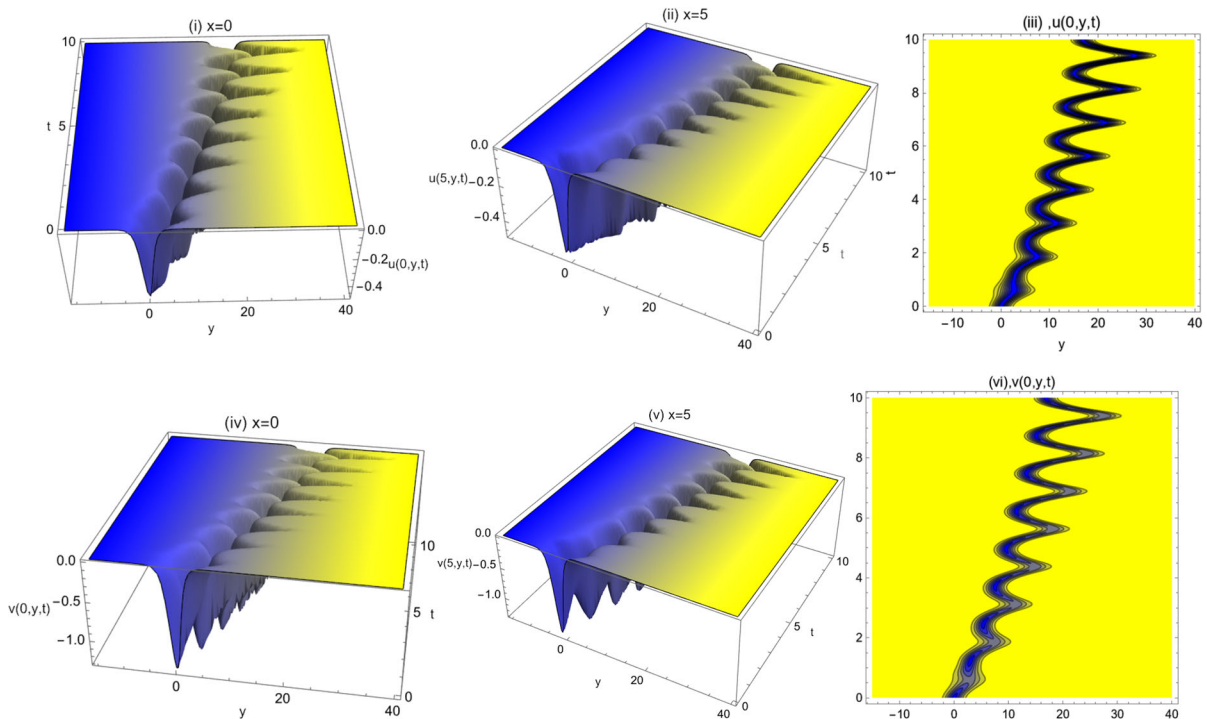$$A(t) = -\frac{60(m - 1)s_0(c_2s_0 - c_1s_1)}{}$$

Fig. 4 Figure 4 (i)-(vi). The 3D and contour plots of u and v are displayed against y and t for two values of x, in Fig. 4(i)–(iii) and (v)–(vi), respectively. When $\alpha(t) = 0.3e^{-0.5t} \sin(5(t-5)) \sin(5(t-5))$, $v(t) = \cos(5(t-5)) + 2$, , $\beta = 0.2$, $\gamma(t) = $

$\sqrt{\cos(5(t-5)) + 2}$, $\beta_2 = 5$, $c_1 = 2.5$, $m_1 = 1.5$, $c_0 = 0.7$, $c_2 = 1.5$, $\beta_3 = 0.3$.

Figure 4(i) and (ii) shows internal dromoions. Figure 4(iii) shows helix-shaped waves.

Figure 4(iv)–(vi) shows the same behavior as in Figs. 4(i)-(iii).

$$(\beta_2 - 30)(a_1 s_0 - a_0 s_1),$$

$$\sigma(t) = -\frac{5\beta_2^3 v(t)\left(4c_2^2 m s_0^2 - 4c_1 c_2 m s_1 s_0 + c_1^2 s_1^2\right)}{(\beta_2 - 30)^2(\beta_2 - 10\beta_3)s_1^2 \gamma(t)},$$

$$h(t) = \frac{1}{K}\left(4c_2^2 m s_0^2 - 4c_1 c_2 m s_1 s_0 + c_1^2 s_1^2\right)^2 \beta_2^5 v(t)$$

$$\left(-100\left(\beta_3^2 \gamma(t)^2\right.\right.$$

$$-15\beta_3 \gamma(t)^2 - 225\alpha(t)v(t))$$

$$+\beta_2^2\left(25\alpha(t)v(t) + 4\gamma(t)^2\right)$$

$$-30\beta_2\left(50\alpha(t)v(t) + (\beta_3 + 5)\,\gamma(t)^2\right)\right),$$

$$K = \beta_1(\beta_2 - 30)^5(\beta_2 - 10\beta_3)^2 s_1^4 \gamma(t)^2. \tag{32}$$

The solution of (5) is

$$\psi(x, y, t) = \frac{P}{Q}, \quad P = -(60(m-1)s_0(c_2 s_0 - c_1 s_1)$$

$$\left(a_0 - \frac{1}{2c_2}a_1\left(c_1 + \sqrt{\frac{4c_2 m s_0(c_2 s_0 - c_1 s_1)}{s_1^2} + c_1^2}\text{Tanh}\right.\right.$$

$$\left[\frac{1}{2}\sqrt{\frac{4c_2 m s_0(c_2 s_0 - c_1 s_1)}{s_1^2} + c_1^2}\right.$$

$$(B(t) - \frac{5\beta_2^3 y v(t)\left(4c_2^2 m s_0^2 - 4c_1 c_2 m s_1 s_0 + c_1^2 s_1^2\right)}{(\beta_2 - 30)^2(\beta_2 - 10\beta_3)s_1^2 \gamma(t)}$$

$$\left.\left.\left.-\frac{\beta_2 x}{\beta_2 - 30}\right)\right]\right)\right),$$

$$Q = (a_1 s_0 - a_0 s_1)(\beta_2 - 30)(s_0 - \frac{1}{2c_2}s_1(c_1 +$$

$$\sqrt{\frac{4c_2 m s_0(c_2 s_0 - c_1 s_1)}{s_1^2} + c_1^2}\text{Tanh}$$

$$\left[\frac{1}{2}\sqrt{\frac{4c_2 m s_0(c_2 s_0 - c_1 s_1)}{s_1^2} + c_1^2}\,(B(t)\right.$$

$$-\frac{5\beta_2^3 y v(t)\left(4c_2^2 m s_0^2 - 4c_1 c_2 m s_1 s_0 + c_1^2 s_1^2\right)}{(\beta_2 - 30)^2(\beta_2 - 10\beta_3)s_1^2 \gamma(t)}$$

$$\left.\left.-\frac{\beta_2 x}{\beta_2 - 30}\right)\right])),$$

$$B(t) = \int_0^t h(s)\,ds, \tag{33}$$

where $h(t)$ is given in (32).

The waves functions u and v are

$$u(x, y, t) = \frac{P_1}{Q_1},$$

$$P_1 = -60(m-1)\text{Sech}\left[\frac{\sqrt{4c_2 m s_0 (c_2 s_0 - c_1 s_1) + c_1^2 s_1^2}}{2s_1}\right.$$

$$\left(B(t) - \frac{5\beta_2^3 y v(t) \left(4c_2^2 m s_0^2 - 4c_1 c_2 m s_1 s_0 + c_1^2 s_1^2\right)}{(\beta_2 - 30)^2 (\beta_2 - 10\beta_3) s_1^2 \gamma(t)}\right.$$

$$\left.\left.- \frac{\beta_2 x}{\beta_2 - 30}\right)\right]^2$$

$$\beta_2 c_2 s_0 (c_2 s_0 - c_1 s_1) \left(4c_2^2 m s_0^2 - 4c_1 c_2 m s_1 s_0 + c_1^2 s_1^2\right),$$

$$Q_1 = s_1^2 (\beta_2 - 30)^2 \left(-2c_2 s_0 + s_1 (c_1\right.$$

$$+ \frac{1}{s_1}\sqrt{4c_2 m s_0 (c_2 s_0 - c_1 s_1) + c_1^2 s_1^2}$$

$$\text{Tanh}\left[\frac{\sqrt{4c_2 m s_0 (c_2 s_0 - c_1 s_1) + c_1^2 s_1^2}}{2s_1}\right.$$

$$\left(B(t) - \frac{5\beta_2^3 y v(t) \left(4c_2^2 m s_0^2 - 4c_1 c_2 m s_1 s_0 + c_1^2 s_1^2\right)}{(\beta_2 - 30)^2 (\beta_2 - 10\beta_3) s_1^2 \gamma(t)}\right.$$

$$\left.\left.\left.- \frac{\beta_2 x}{\beta_2 - 30}\right)\right]\right)\right)^2, \tag{34}$$

$$v(x, y, t) = \frac{P_2}{\gamma(t) (\beta_2 - 30) s_1^2 Q_1},$$

$$P_2 = -300(m-1)\text{Sech}\left[\frac{1}{2}\sqrt{\frac{4c_2 m s_0 (c_2 s_0 - c_1 s_1)}{s_1^2} + c_1^2}\right.$$

$$\left.\left(B(t) - \frac{5\beta_2^3 y v(t) \left(4c_2^2 m s_0^2 - 4c_1 c_2 m s_1 s_0 + c_1^2 s_1^2\right)}{(\beta_2 - 30)^2 (\beta_2 - 10\beta_3) s_1^2 \gamma(t)} - \frac{\beta_2 x}{\beta_2 - 30}\right)\right]^2$$

$$\beta_2^3 c_2 s_0 (c_2 s_0 - c_1 s_1) v(t) \left(4c_2^2 m s_0^2 - 4c_1 c_2 m s_1 s_0 + c_1^2 s_1^2\right)^2. \tag{35}$$

The functions u and v given in (34) and (35) are displayed in Fig. 5 (i)–(vi).

4.2 When $p = 2$ and $k = 2$

We consider (10) and the AEs

$$g_z(z, t) = \sqrt{c_2 g(z, t)^2 + c_1 g(z, t) + c_0}$$
$$(m_1 g(z, t) + m_0),$$
$$g_t(z, t) = h(t)\sqrt{c_2 g(z, t)^2 + c_1 g(z, t) + c_0}$$
$$(m_1 g(z, t) + m_0). \tag{36}$$

From (10) and (36) into (6), it leads to

$$A'(t) = 0, \quad c_0 = \frac{c_1^2}{4c_2},$$

$$\sigma(t) = -\frac{5 (c_1 m_1 - 2c_2 m_0)^2 v(t)}{32 c_2 \gamma(t)},$$

$$\mu(t) = -\frac{1}{2}, A(t)$$

$$= \frac{\sqrt{3}\sqrt{-\beta_3} s_1^2 \sqrt{2c_2 m_0 - c_1 m_1}\sqrt{2c_2 m_0 - c_1 m_1} (c_1 m_1 - 2c_2 m_0)}{4\beta_3 \sqrt{c_2} s_1 (4a_0 c_2 m_1 - a_1 (2c_2 m_0 + c_1 m_1))},$$

$$h(t) = \frac{(c_1 m_1 - 2c_2 m_0)^4 v(t) \left(25\alpha(t) v(t) + 4\gamma(t)^2\right)}{512 \beta_1 c_2^2 \gamma(t)^2},$$

$$s_0 = \frac{1}{4} s_1 \left(\frac{c_1}{c_2} + \frac{2m_0}{m_1}\right). \tag{37}$$

The solution of (5) is

$$\psi(x, y, t) = \frac{P}{Q}, \quad = \sqrt{3}\sqrt{c_2} m_1 2c_2 m_0 - c_1 m_1$$

$$\left(a_1 (m_0 \exp(\frac{1}{2}\sqrt{c_2} m_0 (B(t)\right.$$

$$- \frac{5y (c_1 m_1 - 2c_2 m_0)^2 v(t)}{32 c_2 \gamma(t)} - \frac{x}{2})$$

$$- c_1 \exp(\frac{c_1 m_1 (B(t) - \frac{5y(c_1 m_1 - 2c_2 m_0)^2 v(t)}{32 c_2 \gamma(t)} - \frac{x}{2})}{2\sqrt{c_2}}))$$

$$+ a_0 (2c_2 \exp(\frac{c_1 m_1 (B(t) - \frac{5y(c_1 m_1 - 2c_2 m_0)^2 v(t)}{32 c_2 \gamma(t)} - \frac{x}{2})}{2\sqrt{c_2}})$$

$$- m_1 \exp\left(\frac{1}{2}\sqrt{c_2} m_0 (B(t)\right.$$

$$\left.\left.- \frac{5y (c_1 m_1 - 2c_2 m_0)^2 v(t)}{32 c_2 \gamma(t)} - \frac{x}{2})\right)\right),$$

$$Q = 2c_2 \exp(\frac{c_1 m_1 (B(t) - \frac{5y(c_1 m_1 - 2c_2 m_0)^2 v(t)}{32 c_2 \gamma(t)} - \frac{x}{2})}{2\sqrt{c_2}})$$

$$+ m_1 \exp\left(\frac{1}{2}\sqrt{c_2} m_0 (B(t) - \frac{5y (c_1 m_1 - 2c_2 m_0)^2 v(t)}{32 c_2 \gamma(t)} - \frac{x}{2})\right)$$

$$\sqrt{-\beta_3} (4a_0 c_2 m_1 - a_1 (2c_2 m_0 + c_1 m_1)), B(t) = \int_0^t h(s) ds. \tag{38}$$

where $h(t)$ is given in (37).

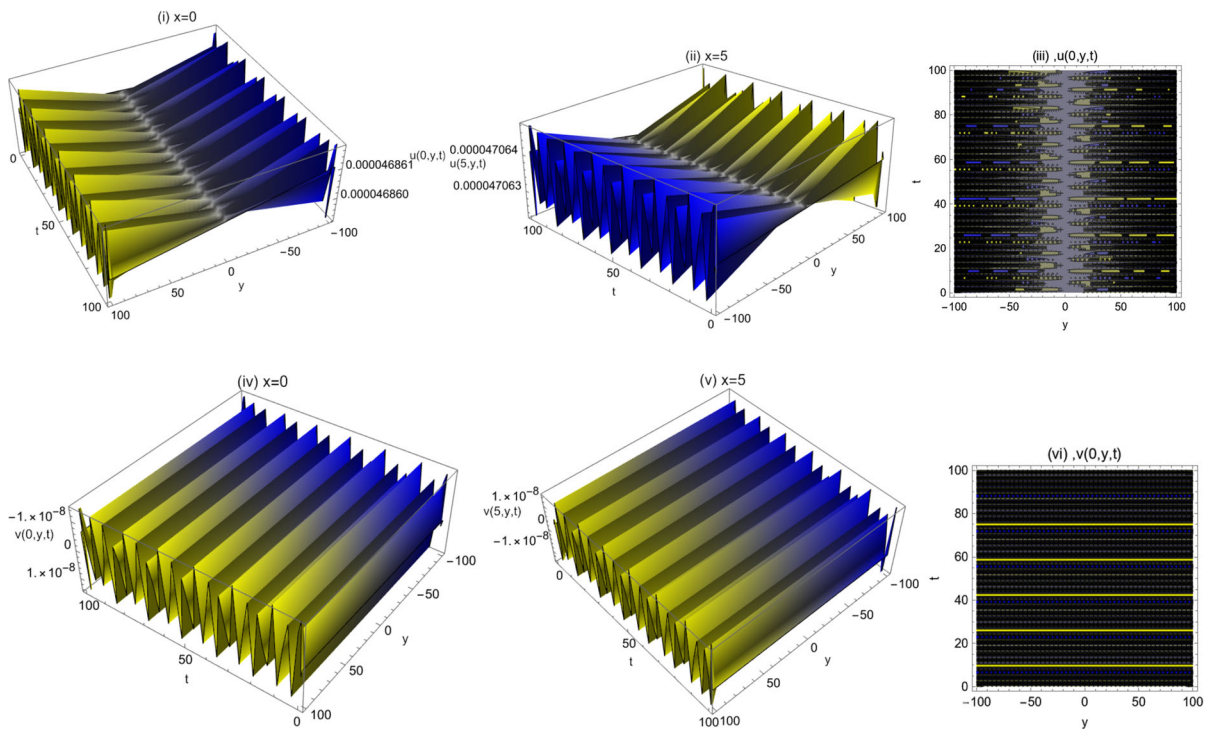The two wave functions u and v are

Fig. 5 Figure 5 (i)–(vi). The 3D and contour plots of u and v are displayed against y and t for two values of x, in Fig. 5(i)–(iii) and (v)-(vi), respectively. When $v(t) = 2\sin(5(t - 5))(\cos(5(t-5))+2.)$, $\alpha(t) = 3e^{-0.3t}\sin(5(t-5))+\cos(5(t - 5))$, $\beta_1 = 0.2$, $\gamma(t) = 0.03\sqrt{\cos(5(t - 5)) + 2}$, $\beta_2 = 0.1$, $c_1 = 0.05$, $c_2 = 0.5$, $\beta_3 = 5$, $s_1 = 1.2$, $s_0 = 0.5$, $m = 0.7$.

Figure 5(i) and (ii) shows waves similar to those created behind and in front of dams. Figure 5 (iii) shows two sets of separated waves.

Figure 5(iv)–(vi) shows doubly periodic waves.

$$u(x, y, t) = \frac{P_1}{Q_1}, \ P_1 = \sqrt{3}m_1\left(c_1m_1 - 2c_2m_0\right)\left(c_1m_1 - c_2m_0\right)$$

$$\exp\left(-\frac{(c_2m_0 + c_1m_1)\left(4c_2\left(4\gamma(t)(x - 2B(t)) - 5c_1m_0m_1yv(t)\right) + 20c_2^2m_0^2yv(t) + 5c_1^2m_1^2yv(t)\right)}{64c_2^{3/2}\gamma(t)}\right),$$

$$Q_1 = 4\sqrt{-\beta_3}(2c_2\exp\left(\frac{c_1m_1(B(t) - \frac{5y(c_1m_1 - 2c_2m_0)^2v(t)}{32c_2\gamma(t)} - \frac{x}{2})}{2\sqrt{c_2}}\right) +$$

$$m_1\exp(\frac{1}{2}\sqrt{c_2}m_0(B(t) - \frac{5y\left(c_1m_1 - 2c_2m_0\right)^2v(t)}{32c_2\gamma(t)} - \frac{x}{2})))^2, \tag{39}$$

$$v(x, y, t) = \frac{P_2}{16c_2\gamma(t)Q_1}, \ P_2 = 5\sqrt{3}m_1\left(c_1m_1 - 2c_2m_0\right)^3\left(c_1m_1 - c_2m_0\right)v(t)$$

$$\exp\left(-\frac{(c_2m_0 + c_1m_1)\left(4c_2\left(4\gamma(t)(x - 2B(t)) - 5c_1m_0m_1yv(t)\right) + 20c_2^2m_0^2yv(t) + 5c_1^2m_1^2yv(t)\right)}{64c_2^{3/2}\gamma(t)}\right). \tag{40}$$

By using (39) and (4), the functions u and v are displayed in Fig. 6 (i)–(vi).

$$\psi(x, y, t) = \frac{(\sqrt{\beta_3(4\beta_3-9)}+2\beta_3)s_0(c_1s_2-c_2s_1)(a_2 B(t)(k_1s_1+k_2s_2)e^{\frac{c_2s_1z}{s_2}}+a_0s_2e^{c_1z})}{\beta_3s_2(a_2s_0-a_0s_2)(B(t)(k_1s_1+k_2s_2)e^{\frac{c_2s_1z}{s_2}}+s_0e^{c_1z})},$$

$$z = -\frac{y\left(15(\sqrt{\beta_3(4\beta_3-9)}+2\beta_3)^2(\sqrt{\beta_3(4\beta_3-9)}+4\beta_3)^2(c_2s_1-c_1s_2)^2v(t)\right)}{8\beta_3^2(2\sqrt{\beta_3(4\beta_3-9)}+4\beta_3-3)^2s_2^2\gamma(t)} - \frac{3x}{2},$$

$$B(t) = \int_0^t h(s)ds,$$

(43)

4.3 Double-wave solutions

In this case, two different AEs are used. We write

$$\varphi(z, t) = \frac{A(t)(a_1g_1(z,t)+a_2g_2(z,t)+a_0)}{s_1g_1(z,t)+s_2g_2(z,t)+s_0},$$

$$g_{1z}(z, t) = c_1g_1(z, t) + c_2g_2(z, t),$$
$$g_{1t}(z, t) = h(t)\left(c_1g_1(z, t) + c_2g_2(z, t)\right),$$
$$g_{2z}(z, t) = d_1g_1(z, t) + d_2g_2(z, t),$$
$$g_{2t}(z, t) = h(t)\left(d_1g_1(z, t) + d_2g_2(z, t)\right).$$

(41)

From (41) into (6), we get

$$A(t) = \frac{1}{\beta_3(a_2s_0-a_0s_2)^2}(2a_2\beta_3s_0^2(c_1s_2-c_2s_1) + 2a_0\beta_3s_2s_0(c_2s_1-c_1s_2)$$

$$-\sqrt{\beta_3(4\beta_3-9)}s_0(a_2s_0-a_0s_2)(c_2s_1-c_1s_2)),$$

$$\sigma(t) = -\frac{15\left(\sqrt{\beta_3(4\beta_3-9)}+2\beta_3\right)^2\left(\sqrt{\beta_3(4\beta_3-9)}+4\beta_3\right)^2(c_2s_1-c_1s_2)^2v(t)}{8\beta_3^2\left(2\sqrt{\beta_3(4\beta_3-9)}+4\beta_3-3\right)^2s_2^2\gamma(t)},$$

$$\mu(t) = -\frac{3}{2}, \; d_2 = -\frac{c_2s_1}{s_2} + c_1 + \frac{d_1s_2}{s_1}, d_1 = \frac{c_2s_1^2-2c_1s_1s_2}{s_2^2}, \; \beta_2 = 30\beta_3,$$

$$h(t) = \frac{P}{Q}, \; P = -\Big(243(2\sqrt{\beta_3(4\beta_3-9)}+4\beta_3-3)^3s_0^5(a_2s_0-a_0s_2)^5$$

$$(c_1s_2-c_2s_1)^9(32\beta_3^2+9+4\left(4\sqrt{\beta_3(4\beta_3-9)}-15\right)\beta_3$$

$$-12\sqrt{\beta_3(4\beta_3-9)})\,v(t)\left(25\alpha(t)v(t)+4\gamma(t)^2\right)\Big),$$

$$Q = 32s_2^4\beta_1\Big(2s_0(a_2s_0-a_0s_2)(c_2s_1-c_1s_2)\sqrt{\beta_3(4\beta_3-9)}+a_2(4\beta_3-3)s_0^2(c_2s_1-c_1s_2)$$

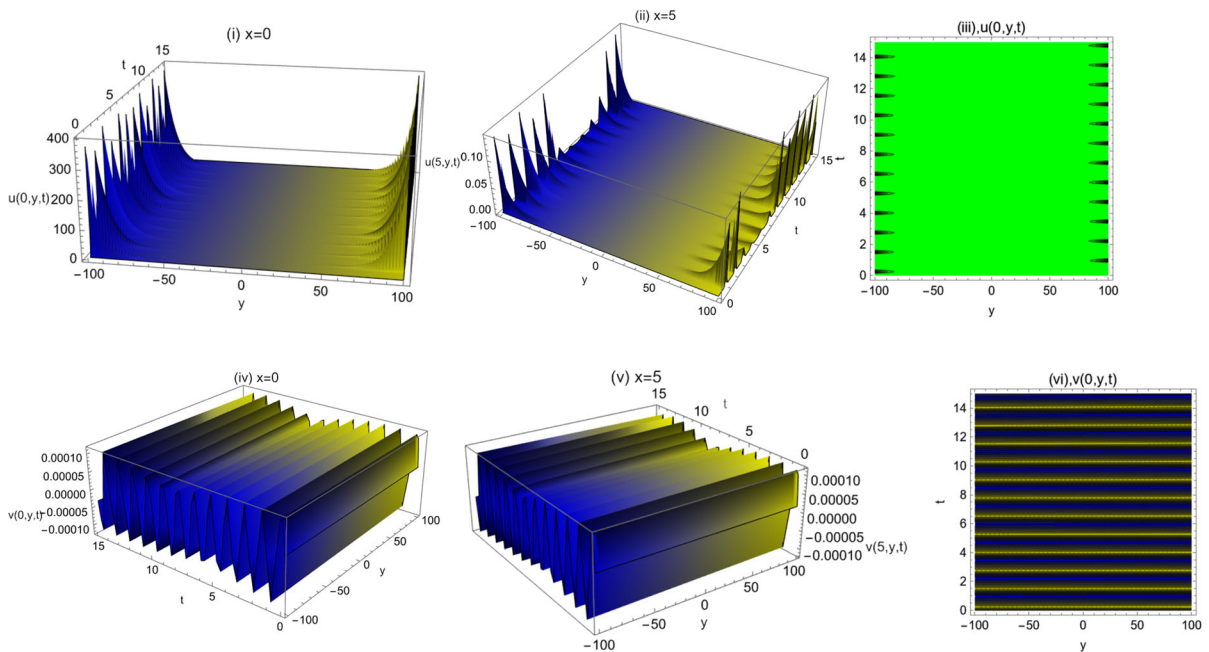$$+ a_0(4\beta_3-3)s_0s_2(c_1s_2-c_2s_1))^5\,\gamma(t)^2\Big).$$

(42)

Fig. 6 Figure 6 (i)–(vi). The 3D and contour plots of u and v are displayed against y and t for two values of x, in Fig. 6(i)–(iii) and (v)-(vi), respectively. When $v(t) = 0.2 \sin(5(t-5))(\cos(5(t-5)) + 2.)$, $\alpha(t) = 0.3e^{-0.3t} \sin(5(t-5)) + \cos(5(t-5))$, $\beta_2 = 0.1, c_2 = 1.5, \beta_3 = -1.5 s_1 = 1.6, s_0 = 1.3, m_1 = 1.2, m_0 = -1.3, \gamma(t) = 3\sqrt{\cos(5(t-5)) + 2}, \beta_1 = 1.3, c_1 = -1.6$.

Figure 6(i) and (ii) shows wave breaking which may occur near barriers, near rocky ocean shores, or near boat sailing. Figure 5 (iii) shows separated waves.

Figure 6(iv)–(vi) shows doubly periodic waves.

where $h(t)$ is given in (42).

The wave functions u and v are

$$u(x, y, t) = \frac{P_1}{Q_1}, \ P_1 = 3 \exp(\frac{1}{8 s_2^3 \gamma(t)} 3(c_2 s_1 + c_1 s_2)(s_2^2(45 c_1^2 y v(t) + 4 x \gamma(t))$$

$$+45 c_2^2 s_1^2 y v(t) - 90 c_1 c_2 s_2 s_1 y v(t)))\left(\sqrt{\beta_3 (4\beta_3 - 9)} + 2\beta_3\right) s_0 B(t) \left(c_2 s_1 - c_1 s_2\right)^2$$

$$\left(k_1 s_1 + k_2 s_2\right), \ Q_1 = 2\beta_3 s_2^2 \left(s_0 \exp(\frac{3 c_2 s_1 \left(s_2^2 \left(45 c_1^2 y v(t) + 4 x \gamma(t)\right) + 45 c_2^2 s_1^2 y v(t) - 90 c_1 c_2 s_2 s_1 y v(t)\right)}{8 s_2^3 \gamma(t)})\right.$$

$$B(t) (k_1 s_1 + k_2 s_2) + \exp(\frac{3 c_1 \left(s_2^2 \left(45 c_1^2 y v(t) + 4 x \gamma(t)\right) + 45 c_2^2 s_1^2 y v(t) - 90 c_1 c_2 s_2 s_1 y v(t)\right)}{8 s_2^2 \gamma(t)})\right)^2, \tag{44}$$

$$v(x, y, t) = \frac{P_2}{4 s_2^2 \beta_3^2 \left(2\sqrt{\beta_3 (4\beta_3 - 9)} + 4\beta_3 - 3\right)^2 \gamma(t) Q_1}, \ P_2 = 15 \exp(\frac{1}{8 s_2^3 \gamma(t)} 3(c_2 s_1 + c_1 s_2)$$

$$(s_2^2(45 c_1^2 y v(t) + 4 x \gamma(t)) + 45 c_2^2 s_1^2 y v(t) - 90 c_1 c_2 s_2 s_1 y v(t))) s_0 B(t)$$

$$\left(c_2 s_1 - c_1 s_2\right)^4 \left(k_1 s_1 + k_2 s_2\right) \left(\sqrt{\beta_3 (4\beta_3 - 9)} + 2\beta_3\right)^3 \left(\sqrt{\beta_3 (4\beta_3 - 9)} + 4\beta_3\right)^2 v(t). \tag{45}$$
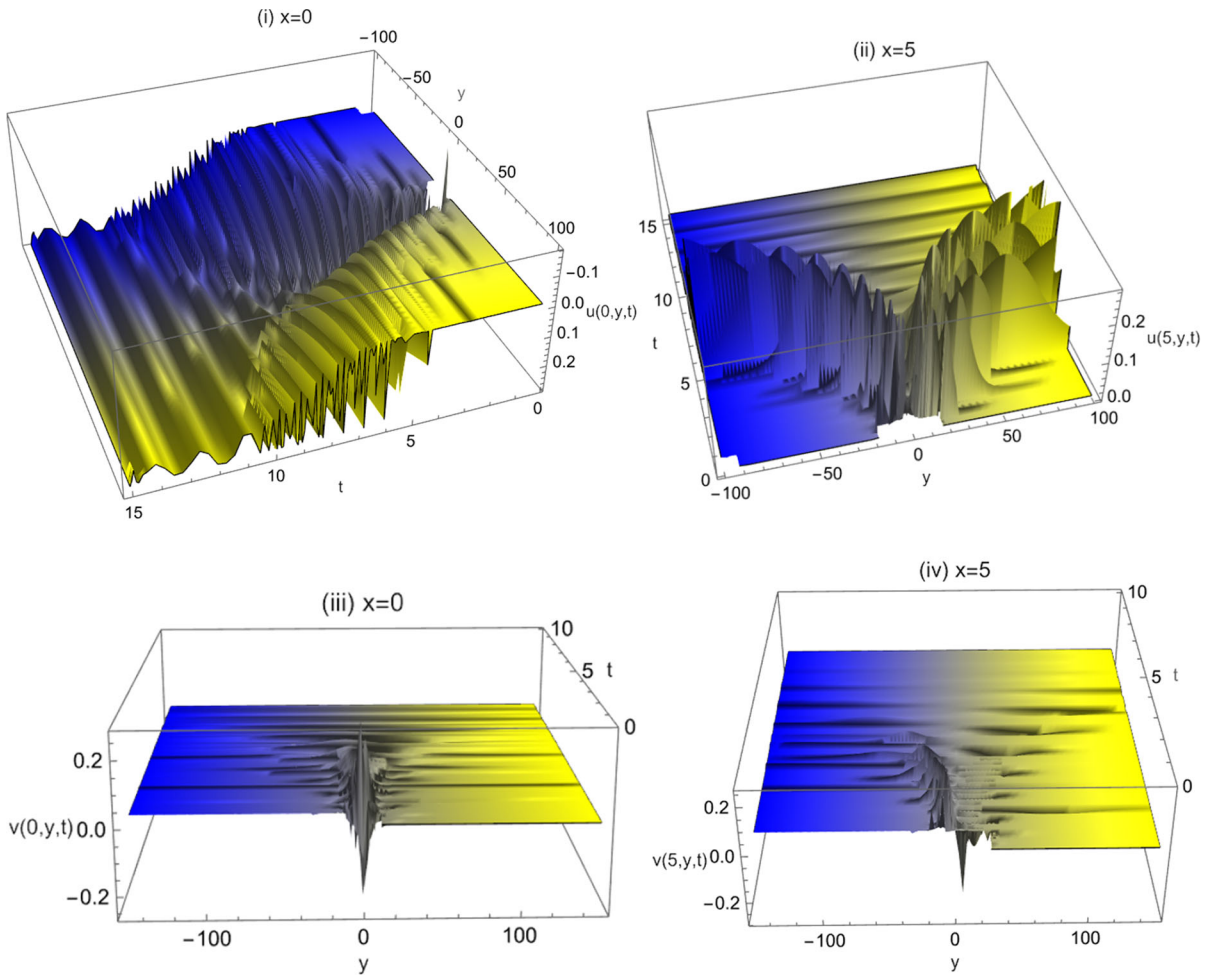
Fig. 7 Figure 7 (i)–(iv). The 3D plots of u and v are displayed against y and t for two values of x, in Figs. 7(i) and (ii) and 6 (iii) and (iv), respectively. When $v(t) = 2\cos(25(t-5))$, $\alpha(t) = 5\sin(15(t-5)) + \cos(15(t-5))$, $s_1 = 0.6$, $s_0 = 0.5$, $\beta_1 = 3$, $c_1 = 0.6$, $c_0 = 0.4$, $a_0 = 2.5$, $a_1 = 0.5$, $a_2 = 2.5$, $\gamma(t) = 3e^{0.5t}$, $\beta_2 = 0.1$, $c_2 = 0.5$, $\beta_3 = 3$, $s_2 = 3$, $k_1 = 1$, $k_2 = 2$.

Figure 7(i) shows different waterfall structures, while 7(ii) shows bulge and internal waves similar to those created by near a barrier (island).

Figure 7(iii) and (iv) shows waves similar to those created near a thin barrier.

Equations (44) and (45) are used to display u and v in Fig. 7(i)–(iv).

5 Discussions

In the present work, multiple different waves structures were found. Attention is focused to simulate these waves to those created in a nonuniform fluid, that is, to waves created near a solid boundary.

(a) Figure 1(i) shows double-U-shape internal (hollowed waves). Figure 1(ii) shows U-shape and S-shape bulge waves.

Figure 1(iv) shows U-shape internal (hollowed wave) and S-shape bulge wave.

(b) Figure 2(i) and (ii) shows waterfalls. Figure 2(iv) shows doubly periodic waves.

Figure 2(iv) and (v) shows towering rogue wave and internal rogue wave (near submarine).

(c) Figure 3(i) and (ii) shows saddle (Fan waves) with periodic waves tail. Figure (iii) shows saddle waves.

Figure 3(iv) and (v) shows periodic waves cascade.

(d) Figure 4(i) and (ii) shows internal dromoions. Figure 4(iii) shows helix-shape waves.

(e) Figure 5(i) and (ii) shows waves similar to those created behind and in front of dams.

(f) Figure 7(i) shows different waterfall structures, while 7(ii) shows bulge and internal waves similar to those created by near a barrier (island).

An experimental work shows rogue wave formation a water tank (which is of solid boundary). This consolidates the results in Fig. 2. Sea also [51].

6 Conclusions

The Caudrey–Dodd–Gibbon–Kotera–Sawada equation is an integro-differential equation that describes two-layer fluid interaction. It was currently studied in the literature when it is with constant coefficients, while, in the non-autonomous version, it was rarely studied. Such equation is of time-dependent coefficients. In the works carried in the literature, in this area, the concepts of two-layer fluid interaction and the notion of nonuniform-fluid were not invoked. Here, these characteristics are taken into consideration. It is shown that the time-dependent coefficients play a crucial role in determining the waves geometry. Here, the later equation version is considered, which describes waves induced by two-layer nonuniform fluid. In this fluid, the velocity is space dependent at a fixed time. It stands for waves created near solid surfaces, boats, dams, networks of (under ground) canals, and submarine. The exact solution of the of the later equation version is found by using the extended unified method, which is a more efficient method when compared with those used in the present case, as it is of lower time cost in symbolic computation. A class of exact solutions are obtained and they are represented graphically. A variety of waves structures are revealed, waves similar to those created, behind and in front of dams, near boat sailing, water fall, and internal waves near submarine. The results found in this paper can be utilized to explain some complex phenomena in oceans and seas. In future works, the extended unified method will be used to investigate waves generated in inhomogeneous or heterogeneous (inhomogeneous-non-uniform) fluids.

Declarations

References

1. Peng, W.Q., Tian, S.F., Zou, L., Zhang, T.T.: Characteristics of the solitary waves and lump waves with interaction phenomena in a (2 + 1)-dimensional generalized Caudrey-Dodd-Gibbon-Kotera-Sawada equation. Nonlinear Dyn. **93**, 1841–1851 (2018)
2. Hu, X.B., Li, Y.: Some results on the Caudrey–Dodd–Gibbon–Kotera–Sawada equation. J. Phys. A: Math. Gen. **24**, 3205 (1991)
3. Ma, H., Yue, S., Deng, A.: Resonance Y-shape solitons and mixed solutions for a (2+1)-dimensional generalized Caudrey-Dodd-Gibbon-Kotera-Sawada equation in fluid mechanics. Nonlinear Dyn. **108**, 505–519 (2022)
4. Zhang, R.F., Li, M.C., Albishari, M., Zheng, F.C., Lan, Z.Z.: Generalized lump solutions, classical lump solutions and rogue waves of the (2+1)-dimensional Caudrey-Dodd-Gibbon-Kotera-Sawada-like equation. Appl. Math. Comput. **403**(15), 126201 (2021)
5. Ma, H., Yue, S., Deng, A.: Nonlinear superposition between lump and other waves of the (2+1)-dimensional generalized Caudrey-Dodd-Gibbon-Kotera-Sawada equation in fluid dynamics. Nonlinear Dyn (2022)
6. Fang, T., Gao, C.N., Wang, H., Wang, Y.H.: Lump-type solution, rogue wave, fusion and fission phenomena for the (2+1)-dimensional Caudrey-Dodd-Gibbon-Kotera-Sawada equation. Mod. Phys. Lett. B **33**(18), 1950198 (2019)
7. Deng, Z.H., Chang, X., Tan, J.N., et al.: Characteristics of the Lumps and Stripe Solitons with Interaction Phenomena

in the (2+1)-Dimensional Caudrey-Dodd-Gibbon-Kotera-Sawada Equation. Int. J. Theor. Phys. **58**, 92–102 (2019)

8. Geng, X., He, G., Wu, L.: Riemann theta function solutions of the Caudrey-Dodd-Gibbon-Sawada-Kotera hierarchy. J. Geom. Phys. **140**, 85–103 (2019)

9. Baskonus, H.M., Mahmud, A.A., Muhamad, K.A., Tanriverd, T.: A study on Caudrey-Dodd-Gibbon-Sawada-Kotera partial differential equation. Math. Meth. Appl. Sci (2022). https://doi.org/10.1002/mma.8259

10. Xu, X.G., Meng, X.H., Zhang, C.Y., GaoY, T.: Analytical investigation of Caudrey-Dodd-GIibon-Kotera-Sawada equation using symbolic computation. Int. J. Mod. Phys. BVol. **27**(06), 1250124 (2013)

11. Chen, J., Li, Y.: M-lump and lump-kink solutions of (2 + 1)-dimensional Caudrey-Dodd-Gibbon-Kotera-Sawada equation. Pramana J. Phys. **94**, 105 (2020)

12. Tariq, H., Ahmed, H., Rezazadeh, H., Javeede, S., Alimgeer, K.S., Nonlaopong, K., Bailihi, J., Khedher, K.M.: New travelling wave analytic and residual power series solutions of conformable Caudrey-Dodd-Gibbon-Sawada-Kotera equation. Res. Phys. **29**, 104591 (2021)

13. Yusuf, A., Sulaiman, T.A., Inc, M., Bayram, M.: Breather wave, lump-periodic solutions and some other interaction phenomena to the Caudrey-Dodd-Gibbon equation. Eur. Phys. J. Plus **135**, 563 (2020)

14. Baleanu, D., Inc, M., Yusuf, A., Aliy, A.I.: Lie symmetry analysis, exact solutions and conservation laws for the time fractional Caudrey-Dodd-Gibbon-Sawada-Kotera equation. Commun. Nonlinear Sci. Num. Simul. **59**, 222–234 (2018)

15. Aiyer, R.N., Fuchssteiner, B., Oevel, W.: Solitons and discrete eigenfunctions of the recursion operator of non-linear evolution equations. I. The Caudrey-Dodd-Gibbon-Sawada-Kotera equation. J. Phys. A: Math. Gen. **19**, 3755 (1986)

16. Na, L., Jian-Qin, M., Hong-Qing, Z.: Symmetry reductions and group-invariant solutions of (2 + 1)-dimensional Caudrey-Dodd-Gibbon-Kotera-Sawada equation. Commun. Theor. Phys. **53**, 591 (2010)

17. Hu, X.B., Zhu, Z.N., Wang, D.L.: A differential-difference Caudrey-Dodd-Gibbon-Kotera-Sawada equation. J. Phys. Soc. Jpn. **69**, 1042–1049 (2000)

18. Lia, L., Xie, Y., Wang, M.: Characteristics of the interaction behavior between solitons in (2+1)-dimensional Caudrey-Dodd-Gibbon-Kotera-Sawada equation. Res. Phys. **19**, 103697 (2020)

19. Liu, S.H., Tian, B.: Singular soliton, shock-wave, breather-stripe soliton, hybrid solutions and numerical simulations for a (2+1)-dimensional Caudrey-Dodd-Gibbon-Kotera-Sawada system in fluid mechanics. Nonlinear Dyn. **108**, 2471–2482 (2022)

20. Wazwaz, A.M.: Multiple-soliton solutions for the fifth order Caudrey-Dodd-Gibbon (CDG) equation. Appl. Math. Comput. **197**(2), 719–724 (2008)

21. Cheng, X.P., Wang, J.Y., Ren, B., Yun-Qing Yang, Y.Q.: Interaction behaviours between solitons and cnoidal periodic waves for (2+1)-dimensional Caudrey–Dodd–Gibbon–Kotera–Sawada equation. Commun. Theor. Phys. **66**, 163 (2016)

22. Cheng, X., Yang, Y., Renc, B., Wan, J.: Interaction behavior between solitons and (2+1)-dimensional CDGKS waves. Wave Motion **86**, 150–161 (2019)

23. Yang, S., Zhang, Z.,1 and Li B.,Soliton Molecules and Some Novel Types of Hybrid Solutions to (2+1)-Dimensional Variable-Coefficient Caudrey-Dodd-Gibbon-Kotera-Sawada Equation, Adv. Math. Phys. 2020 |Article ID 2670710 (2020)

24. Liu, F.Y., Gao, Y.T., Yu, X., Hu, L., Wu, X.H.: Hybrid solutions for the (2+1)-dimensional variable-coefficient Caudrey-Dodd-Gibbon-Kotera-Sawada equation in fluid mechanics. Chaos, Solitons Fractals **152**, 111355 (2021)

25. Manafian, J., Lakestan, M.: N-lump and interaction solutions of localized waves to the (2+1)-dimensional variable-coefficient Caudrey-Dodd-Gibbon-Kotera-Sawada equation. J. Geom. Phys. **150**, 103598 (2020)

26. Liu, D., Ju, X., Ilhan, O.A., Manafian, J., Farhan, H.: Ismael Multi-Waves, Breathers, Periodic and Cross-Kink Solutions to the (2+1)-Dimensional Variable-Coefficient Caudrey-Dodd-Gibbon-Kotera-Sawada Equation. J. Ocean Univ. China **20**, 35–44 (2021)

27. Cheng, W. G., Li, B. , Chen, Y.: Bell Polynomials Approach Applied to (2 + 1)-Dimensional Variable-Coefficient Caudrey-Dodd-Gibbon-Kotera-Sawada Equation, Abs. Appl. Ana. 2014 |Article ID 523136 (2014)

28. Li, J., Manafian, J. ,Wardhana, A. , Othman, A. J., Husein, I., Al-Thamir, M., Abotaleb, M.: N-Lump to the (2+1)-Dimensional Variable-Coefficient Caudrey-Dodd-Gibbon-Kotera-Sawada Equation, Complexity 2022 |Article ID 4383100 (2022)

29. Ghanbari, B., Asadi, E.: New solitary wave solutions of the Sawada-Kotera equation and its bidirectional form. Phys. Scr. **96**, 104011 (2021)

30. Deng, G.F., Gao, Y.T., Su, J.J., Ding, C.C., Ji, T.T.: Solitons and periodic waves for the (2 + 1)-dimensional generalized Caudrey-Dodd-Gibbon-Kotera-Sawada equation in fluid mechanics. Nonlinear Dyn. **99**, 1039–1052 (2020)

31. Yang, S., Zong-Hang, Y.: A series of exact solutions of (2+1)-dimensional CDGKS Equation. Commun. Theore. Phys. **46**(5), 807–811 (2006)

32. Zhang, R.F., Li, M.C., Albishari, M., Zheng, F.C., Lan, Z.Z.: Generalized lump solutions, classical lump solutions and rogue waves of the (2+1)-dimensional Caudrey-Dodd-Gibbon-Kotera-Sawada-like equation. Applied Math. Comput. **403**, 126201 (2021)

33. Zhang, R.F., Li, M.C.: Bilinear residual network method for solving the exactly explicit solutions of nonlinear evolution equations. Nonlinear Dyn. **108**, 521–531 (2022)

34. Wazwaz, A.: Integrable (3+1)-dimensional Ito equation: variety of lump solutions and multiple-soliton solutions. Nonlinear Dyn. (2022). https://doi.org/10.1007/s11071-022-07517-0

35. Wazwaz, A.: Derivation of lump solutions to a variety of Boussinesq equations with distinct dimensions. Int. J. Numer. Methods Heat Fluid Flow (2022). https://doi.org/10.1108/HFF-12-2021-0786

36. Abdel- Gawad, H.I., Elazab, N. S., Osman, M.: Exact solutions of space dependent Korteweg-de Vries equation by the extended unified method. J. Phys. Soc. Japan 82, 044004 (2013)

37. Abdel-Gawad, H.I.: Self-steepening, Raman scattering and self-phase modulation-interactions via the perturbed Chen-Lee-Liu equation with an extra dispersion. Modulation ins-

ability and spectral analysis. Opt. Quant. Elec. **54**, 426 (2022). https://doi.org/10.1007/s11082-022-03773-x

38. Abdel-Gawad, H.I.: Longitudinal-transverse soliton chains analog to Heisenberg ferromagnetic spin chains in (2+1) dimensional with biquadrant interaction. Opt. Quant. Elect. **54**, 479 (2022). https://doi.org/10.1007/s11082-022-03860-z

39. Abdel-Gawad, H.I.: Intricate and multiple chirped waves geometric structures solutions of two-mode KdV equation, spectral and stability analysis. Int. J. Mod. Phys. B **36**(14), 2250056 (2022)

40. Abdel-Gawad, H. I., Aldailami, A. A., Saad, K. M., Gómez-Aguilar, J. F.: Numerical solution of q-dynamic equations, Numer Meth. P. D. Eq.38, 1162-1179 (2022)

41. Zhang, R.F., Li, M.C.: Bilinear residual network method for solving the exactly explicit solutions of nonlinear evolution equations. Nonlinear Dyn. **108**, 521–531 (2022)

42. Ma, H., Gao, Y., Deng, A.: Fission and fusion solutions of the (2+1)-dimensional generalized Konopelchenko-Dubrovsky-Kaup-Kupershmidt equation: case of fluid mechanics and plasma physics. Nonlinear Dyn. **108**, 4123–4137 (2022)

43. Li, B.Q., Ma, Y.: N-order rogue waves and their novel colliding dynamics for a transient stimulated Raman scattering system arising from nonlinear optics. Nonlinear Dyn. **101**, 2449–2461 (2020)

44. Ma, Y.L., Wazwaz, A.M., Li, B.Q.: New extended Kadomtsev-Petviashvili equation: multiple soliton solutions, breather, lump and interaction solutions. Nonlinear Dyn. **104**, 1581–1594 (2021)

45. Li, B.Q., Ma, Y.L.: Interaction dynamics of hybrid solitons and breathers for extended generalization of Vakhnenko equation. Nonlinear Dyn. **102**, 1787–1799 (2020)

46. Ma, Y.L., Wazwaz, A.M., Li, B.: Q, A new (3+1)-dimensional Kadomtsev-Petviashvili equation and its integrability, multiple-solitons, breathers and lump waves. Math. Comput. Simul. **187**, 505–519 (2021)

47. Gupta, V., Mittal, M., Mittal, V.: Chaos theory: an emerging tool for arrhythmia detection. Sens Imaging **21**, 10 (2020)

48. Peng, Z.W., Yu, W.X., Wang, J.N., Wang, J., Chen, Y., He, X.K., Jiang, D.: Dynamic analysis of seven-dimensional fractional-order chaotic system and its application in encrypted communication. J. Ambient Intell. Hum. Comput. **11**, 5399–5417 (2020)

49. Rigatos, G., Siano, P., Zervos, N.: An approach to fault diagnosis of nonlinear systems using neural networks with invariance to Fourier transform. J. Ambient Intell. Hum. Comput. **4**, 621–639 (2013)

50. Guo, J. l., Chen, Y. Q., Lai, G. y., Liu, H. l., Tian, Y., Al-Nabhan, N., Wang, J., Wang, Z.: Neural networks-based adaptive control of uncertain nonlinear systems with unknown input constraints. J. Ambient Intell. Hum. Comput. (2021)

51. A. Wang A. Ludu A., Zong Z., L. Zou L., and Pei Y., Experimental study of breathers and rogue waves generated by random waves over non-uniform bathymetry, Phys. Fluids 32, 087109 (2020)